Local-field effects on the near-surface and near-interface screened electric field in noble metals

L. Calmels*
Research Institute for Materials, University of Nijmegen, Toernooiveld 1, 6525 ED Nijmegen, The Netherlands
Department of Physics and Astronomy, University of Wales, PO Box 913, Cardiff CF24 3YB, United Kingdom

J. E. Inglesfield
Department of Physics and Astronomy, University of Wales, PO Box 913, Cardiff CF24 3YB, United Kingdom

E. Arola† and S. Crampin
Department of Physics, University of Bath, Bath BA2 7AY, United Kingdom

Th. Rasing
Research Institute for Materials, University of Nijmegen, Toernooiveld 1, 6525 ED Nijmegen, The Netherlands
(Received 24 September 2000; revised manuscript received 28 March 2001; published 10 September 2001)

The screening of an optical electric field at a noble metal surface is evaluated within a semiclassical model where the nonlocality of the *d*-electron response is taken into account via a set of interacting atomic dipoles. The dipole moments in the first few atomic layers differ from the expected bulk value due to the symmetry breakdown at the surface. These effects give rise to surface-induced electric charges and currents and to a surface-induced electric field which vanishes in the bulk but can be important in the top atomic layers. This field takes into account local-field effects, is frequency dependent and is strongly enhanced in a frequency range characteristic of the metal surface. Results are first given for an electric field perpendicular to the metal surface, and the enhancement of the surface response is mainly due to interband electronic transitions for the Cu and Au surfaces, while it originates from a coupling with the bulk plasmon excitations for an Ag surface. The anisotropy in the surface response is studied for an electric field parallel to the anisotropic Ag(110) surface. Finally, the calculation is generalized to describe screening effects at an interface between two different noble metals. The simple surface model used in this paper shows that the surface-induced electric field should be taken into account in the simulations of surface spectroscopy, where the calculated signal directly depends on the linearly screened field at the surface.

DOI: 10.1103/PhysRevB.64.125416 PACS number(s): 78.20.Bh, 78.66.Bz, 73.20.Mf

I. INTRODUCTION

The response of a metallic system to an external electric field is greatly influenced by the presence of the surface. The surface effects manifest themselves as surface charge and current densities which take place in a finite but thin region due to the efficiency of screening processes in metals. Typically, the effective surface thickness is smaller than the wavelength of any external optical probe and will lead to nonlocal optical effects which can be measured in experiments and modify surface and interface spectroscopies. For a detailed review on electronic excitations at metal surfaces, see Ref. 1; for a general review of the theory of surface optical properties, see Refs. 2 and 3.

Experimental evidence of the surface-induced effects was observed a long time ago in optical measurements such as reflection spectroscopy, reflectance anisotropy spectroscopy, and ellipsometry. These optical experiments are related to the field far from the surface and it has been shown that the electromagnetic wave reflected at a metal surface presents deviations from the classical Fresnel fields.[4] These deviations have been formulated within the so-called ''*d*-parameter'' theory[5] or within several other equivalent formalisms.[6] The *d*-parameter theory simply describes the reflected and transmitted electromagnetic waves with two simple parameters which are directly related to the parallel and perpendicular surface-induced current densities and to the surface collective excitations (surface plasmons). The *d*-parameter and equivalent formalisms have been intensively used to study different simple models of insulating[7,8] and metallic[9–14] surfaces. It has also been extended in order to study optical properties at a general interface.[15]

Surface screening is an important concept to describe the field far from the surface but it also strongly modifies the near-surface characteristics. The knowledge of the near-surface electric field will be useful for analyzing surface experiments such as photoemission or second harmonic generation spectroscopies, in which the measured signal is determined by the local electric field as well as by the surface electronic structure. These experimental methods are widely used to investigate surface properties and an important theoretical effort has been made to analyze experimental data.[16] While the surface response functions have been intensively investigated, for instance via first principles calculations of the surface electronic structure, an accurate description of the near-surface electric field is often neglected.

The near-surface electric field has been extensively studied in the literature within the jellium approximation.[5,9,10] The jellium model has been studied to describe the screening properties of both static and dynamic electric fields. This model is suitable for describing simple alkali metals where the screening process mainly comes from nearly-free *sp* elec-

trons but it becomes less realistic for the case of noble metals where the localized *d* electrons also play an important role. The screening properties of the *d* electrons have been taken into account to study the field far from the surface,[12–14] but few attempts have been made to describe their effects on the near-surface field. A simple model including partial local-field effects has for instance been used recently,[17] but this model neglects the crystal periodicity in directions parallel to the surface.

Our aim in the present paper is to use a semiclassical model which takes into account the *d*-electron screening properties and their associated local-field effects to calculate the near-surface electric field in noble metal systems. We use the model of Tarriba and Mochán[12] which they used to calculate the field far from an Ag surface. It has given results for the optical reflectance anisotropy spectra of an Ag(110) surface in very good agreement with experimental data.[13]

Our paper is organized as follows. In Sec. II we describe the surface model and the theory used to calculate the near-surface electric field. We apply this theory in Sec. III to study the comparatively simple Cu(110), Au(110), and Ag(110) surfaces and we first investigate the frequency dependence of the surface response when the applied electric field is perpendicular to the surface. We then describe the anisotropy of the surface response when the field is applied parallel to the surface. In Sec. IV we briefly show how the model can be extended to describe screening at metallic interfaces. We discuss our results and draw conclusions in Sec. V.

II. MODEL OF THE SURFACE RESPONSE

We use the semiclassical model of a transition metal surface described by Tarriba and Mochán.[12] The metal with a surface is described by a semi-infinite lattice of N polarizable atomic spheres per unit volume immersed in semi-infinite free-electron jellium. As the electromagnetic wavelength and penetration depth in the metal are large compared to the distance over which surface effects take place, we can work in the long-wavelength limit and consider the charge response of the system to the applied electric field.

The nearly free electron jellium is described by the Drude dielectric function

$$\epsilon_{\mathrm{D}}(\omega)=1-\frac{\omega_{\mathrm{DP}}^2}{\omega(\omega+i/\tau)}, \tag{1}$$

where ω_{DP} and τ are, respectively, the Drude bulk plasmon frequency and the collision time which characterize the sp electrons. In noble metals these parameters can be fitted to the low frequency behavior of the measured dielectric function $\epsilon(\omega)$,[18,19] since in these systems there is a clear separation between a free-electron frequency regime and the onset of interband transitions, and as $\omega\to 0$ we have $\epsilon\approx\epsilon_{\mathrm{D}}$.

The polarizable atomic spheres take into account the response of the *d* electrons and *sp* electrons within the spheres. Following Tarriba and Mochán[12] we assume that all the atomic sites are characterized by the same polarizability α, which can be found from the measured bulk ϵ

$$\alpha=\frac{3}{4\pi N}\frac{\epsilon-\epsilon_{\mathrm{D}}}{\epsilon+2\epsilon_{\mathrm{D}}}. \tag{2}$$

This follows from the Lorentz-Lorenz relation.[20] The dipole moment of atomic spheres in atomic layer n is then given by

$$\mathbf{p}(n)=\alpha(\omega)\mathbf{E}_{\mathrm{loc}}(n), \tag{3}$$

where $\mathbf{E}_{\mathrm{loc}}(n)$ is the local electric field.

We now explain the calculation of the electric field in the semi-infinite metal. The sharp jellium edge is at $z=0$, with the metal located at $z>0$ and vacuum at $z<0$; the first atomic layer is at a distance $d/2$ from the jellium edge, where d is the interlayer spacing, and the origins of the axes are chosen so that an atom in the first layer is located at $x=0$, $y=0$, $z=d/2$. We first consider the field with only the jellium present, with no polarizable atoms. The electric field is then given by

$$\mathbf{E}_0=(E_{\mathrm{ext},x};E_{\mathrm{ext},y};E_{0z})\exp(i\omega t), \tag{4}$$

with $E_{0z}=E_{\mathrm{ext},z}$ on the vacuum side and $E_{0z}=E_{\mathrm{ext},z}/\epsilon_{\mathrm{D}}$ on the jellium side. We now add on to this ''applied'' field the contribution due to the atomic dipoles immersed in the jellium. From the method of images, the microscopic electric field at point $\mathbf{r}$ in the metal is given by

$$\mathbf{E}(\mathbf{r})=\mathbf{E}_0+\sum_n \mathsf{S}(\mathbf{r},n)\cdot\mathbf{p}(n)+\frac{\epsilon_{\mathrm{D}}-1}{\epsilon_{\mathrm{D}}+1}\sum_n \mathsf{S}(\mathbf{r},-n)\cdot\mathbf{p}'(n). \tag{5}$$

The first summation is over the layers of atoms, and the tensor $\mathsf{S}(\mathbf{r},n)$ gives the electric field at point $\mathbf{r}$ due to all the dipoles in the nth layer. The second summation gives the contribution from the image dipoles, and $\mathsf{S}(\mathbf{r},-n)$ gives the field due to the image of layer n located at $-z_n$; the dipole itself is reflected, so that $\mathbf{p}'=(p_x;p_y;-p_z)$. The numerical methods used to perform the summation over a layer of point dipoles to calculate S have been described previously, and S has been obtained for different crystal structures.[21–23] The microscopic field at point $\mathbf{r}$ in the vacuum is similarly given by

$$\mathbf{E}(\mathbf{r})=\mathbf{E}_0+\frac{2\epsilon_{\mathrm{D}}}{\epsilon_{\mathrm{D}}+1}\sum_n \mathsf{S}(\mathbf{r},n)\cdot\mathbf{p}(n). \tag{6}$$

These equations have previously been derived in Ref. 12.

The dipole moments in each layer can be found from Eqs. (2) and (3), evaluating from Eq. (5) the local field $\mathbf{E}_{\mathrm{loc}}(\mathbf{r}_n)$ in the center of the atomic spheres, but excluding the dipole contribution from the atom under consideration. These constitute a set of linear equations in $\mathbf{p}(n)$ in terms of the applied field, which can be solved by matrix inversion. To obtain a finite set of equations we assume the bulk value of the dipole moment beyond a certain layer (typically 20 or 30 layers). A simplifying feature of the calculation, when the point dipoles are located at high symmetry points for a cubic crystal such as Cu, Ag, or Au, is that each component of the dipole moments only depends on the corresponding component of the applied field, S being a diagonal tensor.

Deep in the bulk we can neglect the contribution from the image charges in Eq. (5), and the dipole moments can be taken as identical for all the layers. The local electric field at an atomic site away from the surface $\mathbf{r}_{\text{bulk}}$ is then given by

$$\mathbf{E}_{\text{loc}}(\mathbf{r}_{\text{bulk}}) = \mathbf{E}_0 + \left(\sum_n{}' \, \mathsf{S}(\mathbf{r}_{\text{bulk}}, n) \right) \cdot \mathbf{p}_{\text{bulk}}, \tag{7}$$

where the prime on the summation indicates that the contribution to S from the atomic site itself is excluded. For the x and y components (parallel to the surface) of electric fields and dipole moments, it can be shown that the summation over layers gives[8]

$$\left(\sum_n{}' \, \mathsf{S}(\mathbf{r}_{\text{bulk}}, n) \right)_{xx,yy} = \frac{4\pi N}{3}, \tag{8}$$

and for the z component (perpendicular to the surface)

$$\left(\sum_n{}' \, \mathsf{S}(\mathbf{r}_{\text{bulk}}, n) \right)_{zz} = -\frac{8\pi N}{3}. \tag{9}$$

We have checked that our values for the layer summations obey these sum rules. The bulk dipole moments are then given by Eq. (3), with the following local field components:

$$E_{\text{loc},x(y)}(\mathbf{r}_{\text{bulk}}) = \frac{E_{\text{ext},x(y)}}{1 - 4\pi N\alpha/3}, \quad E_{\text{loc},z}(\mathbf{r}_{\text{bulk}}) = \frac{E_{\text{ext},z}/\epsilon}{1 - 4\pi N\alpha/3}. \tag{10}$$

These are of course the local fields from Lorentz-Lorenz.[20]

The expression for the electric field given by Eq. (5), with point dipoles at each atomic site, breaks down if we want the electric field *within* an atom. This is needed for calculating optical matrix elements, for example. Inside the atom centered at $\mathbf{r}_n$, we must remove the divergent contribution to Eq. (5) from the local dipole $\mathbf{p}(n)$, and replace it by the field from the polarized atomic charge, setting the dipole moment of the polarized atom equal to $\mathbf{p}(n)$.

We choose to represent the polarized atom by a small uniform shift of its *d*-electron charge density, given in terms of the Roothaan-Hartree-Fock atomic wave functions by[24]

$$\rho(r) = \sum_n N_n r^{\alpha_n} \exp(-\beta_n r). \tag{11}$$

The coefficients N_n, α_n, and β_n can be obtained from the tabulated wave functions.[24] We consider a translation of the *d*-electron charge density by a small vector $\mathbf{u}$ in the z direction. This translation gives rise to a dipole moment $\mathbf{p} = Q\mathbf{u}$, where Q is the total *d*-electron charge. In a system of Cartesian coordinates centered on the polarized atom, the corresponding electric field takes the form

$$\mathbf{E}_{\text{atom}}(\mathbf{r}) = p\left\{ E_1(r)\left(\frac{xz}{r^2}\mathbf{e}_x + \frac{yz}{r^2}\mathbf{e}_y + \frac{z^2}{r^2}\mathbf{e}_z \right) + E_2(r)\mathbf{e}_z \right\}, \tag{12}$$

where the functions $E_1(r)$ and $E_2(r)$ can be derived easily from Eq. (11). At any point $\mathbf{r}$ inside the metal, we use this expression to find the contribution to the field from the closest atoms (those with significant charge at $\mathbf{r}$), replacing their point dipole fields.

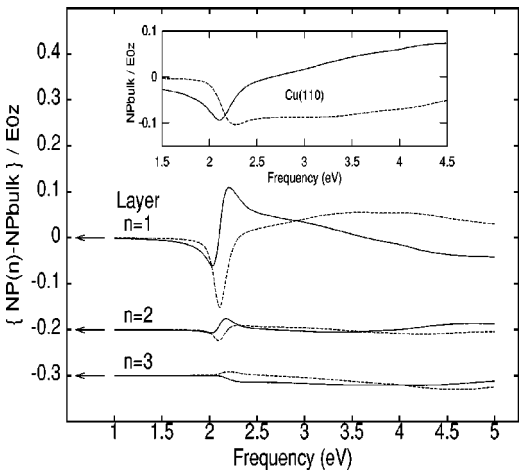

FIG. 1. Real part (solid lines) and imaginary part (dashed lines) of the difference $N[p(n) - p_{\text{bulk}}]$ in units of E_{0z}, for the first ($n=1$), second ($n=2$), and third ($n=3$) atomic layers of a Cu(110) surface in a perpendicular electric field. The results are plotted as a function of the frequency of the applied field. The curves corresponding to different layers have been translated vertically and the offsets are indicated by horizontal arrows. The inset shows the bulk dipole moment Np_{bulk}.

III. RESULTS FOR SIMPLE NOBLE METAL SURFACES

We have calculated the near-surface electric field for several (110) noble metal surfaces. These surfaces are characterized by a relatively small interlayer spacing d and surface effects are for this reason expected to be more important than for the corresponding (100) surfaces. The (110) system is also interesting because the two orthogonal x and y axes parallel to the surface (the $[\bar{1}10]$ and the $[001]$ axes, respectively) define nonequivalent crystallographic directions due to the anisotropic crystallographic structure of these surfaces. We first present results for an external electric field applied perpendicularly to the Cu, Au, and Ag surfaces, and we secondly study the surface response anisotropy for Ag.

A. The Cu(110) surface in a perpendicular electric field

We begin with Cu(110). We have calculated the dipole moments $\mathbf{p}(n) = p(n)\mathbf{e}_z$ corresponding to the external electric field $\mathbf{E}_{\text{ext}} = E_{\text{ext},z}\mathbf{e}_z$, and our results for the first atomic layers strongly depend on the frequency of the external field. The dielectric response is identical for surface and bulk atomic sites at low frequency, but noticeable differences can be observed from about 2.0 eV near the surface. This can be seen in Fig. 1 where $[p(n) - p_{\text{bulk}}]$ is presented for the first few atomic layers. The enhancement of the dipole is most important for the top layer, and the surface effect decreases on moving towards the bulk crystal [the difference between $p(n)$ and p_{bulk} becomes very small over the whole frequency range from the fourth layer]. The strong surface effect shown in Fig. 1 originates from interband electronic transitions

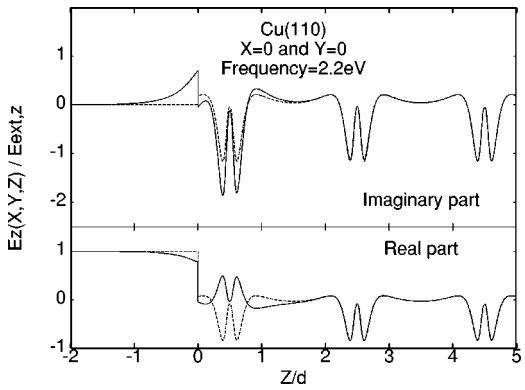

FIG. 2. Real and imaginary parts of the electric field $E_z(x,y,z)$ along a [110] atomic row passing through an atom of the Cu(110) surface layer, for the frequency $\hbar\omega=2.2$ eV. The field, plotted with solid lines as a function of z, is given in units of the external field $E_{\mathrm{ext},z}$ applied perpendicularly to the surface. The dashed lines represent the electric field at an equivalent bulk position if $z>0$, or the external electric field if $z<0$. The jellium edge is located at $z=0$.

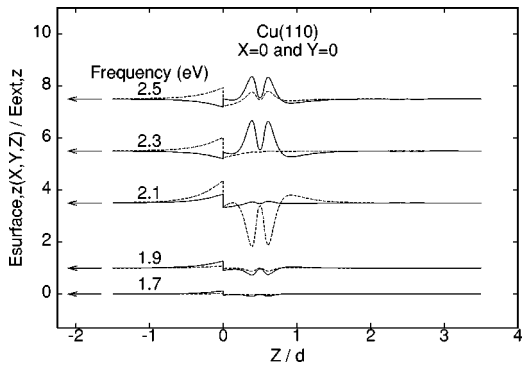

FIG. 3. Real part (solid lines) and imaginary part (dashed lines) of the surface-induced electric field $E_{\mathrm{surface},z}(x,y,z)$ along a [110] atomic row passing through an atom of the Cu(110) surface layer. The field, plotted as a function of z, is given in units of the external field $E_{\mathrm{ext},z}$ applied perpendicularly to the surface, for different values of the frequency. The curves corresponding to different frequencies have been translated vertically and the offsets are indicated by horizontal arrows. The jellium edge is located at $z=0$.

where d-band electrons are excited above the Fermi energy. The interband transition nature of this surface effect can be deduced from the inset in Fig. 1, which gives the frequency dependence of the bulk dipole moment. This shows sharp structure in p_{bulk} at about $\hbar\omega=2.1$ eV, in agreement with the threshold for the interband transition estimated from band structure calculations.[25]

The interband transition will occur at the surface as well as in the bulk. The surface modifications of the electric field are due to the symmetry breakdown at the surface and to the enhancement of the dipole moments in the surface layers. We have calculated the electric fields $\mathbf{E}(\mathbf{r})$ in the vicinity of the Cu surface. The near-surface electric field is a complicated vector with components in x, y, and z directions. However the x and y components of the field have spatial parity properties which are described by Eq. (12); these imply that the field is oriented in the z direction at any point of high xy symmetry. This is, for instance, the case along any [110] atomic row.

As an example of our results, we give in Fig. 2 the z component of the electric field calculated along a [110] atomic row passing through an atom of the first atomic layer ($x=0,y=0$) and corresponding to an external field with frequency $\hbar\omega=2.2$ eV. The general behavior of the electric field can be summarized as follows: the field along this atomic row has strong spatial variations with a complicated shape near the first, third, fifth, . . . , atomic layers located at $z=0.5d$, $2.5d$, $4.5d$, . . . (the line does not pass through any atoms in the even atomic layers). At the jellium edge we obtain continuous variations of the components of the field parallel to the surface while the component perpendicular to the surface presents a discontinuity since $E_z(x,y,z\rightarrow 0^-)=\epsilon_{\mathrm{D}}(\omega)E_z(x,y,z\rightarrow 0^+)$. We observe that the electric field reaches its far-surface value quite rapidly in the vacuum: the electric dipole field is indeed a short range field which vanishes as $1/r^3$ and we obtain $E(x,y,z<0)\approx E_{\mathrm{ext}}$, at a small distance ($z\approx d$) from the jellium edge.

On the metal side, the electric field is strongly disturbed in the vicinity of the first atomic layers and the discrepancy between the calculated field (the solid lines in Fig. 2) and the equivalent bulk field (the dashed lines in Fig. 2) rapidly disappears as z increases: the spatial variation of the field becomes a periodic function of z after a few interlayer distances. For this reason subsequent figures show the ''surface-induced electric field'' $\mathbf{E}_{\mathrm{surface}}(\mathbf{r})$. This field, which corresponds to the difference between the solid and the dashed lines in Fig. 2, gives a direct and precise picture of the short-range dielectric modifications induced by the surface. Of course, the subtraction which gives $\mathbf{E}_{\mathrm{surface}}(\mathbf{r})$ is a somewhat artificial operation and some aspects of the calculated surface-induced field have to be interpreted carefully. For example, the subtraction described above produces a discontinuity in $\mathbf{E}_{\mathrm{surface}}(\mathbf{r})$ at the jellium edge. This discontinuity is purely artificial (a different field is subtracted from the vacuum side and from the metal side)—it occurs for fields parallel as well as for fields perpendicular to the surface—and it is not related to the discrepancy between the jellium and the vacuum dielectric functions.

Figure 3 shows the real and imaginary parts of $E_{\mathrm{surface},z}(\mathbf{r})$ along the same [110] atomic row passing through an atom of the first atomic layer, and for different frequencies. We see that the surface-induced effects are already negligible by the third atomic layer. The frequency dependence of the surface-induced field is somewhat complicated. Close to an atom of the first layer, the surface-induced electric field is negligible in the nearly static limit. The real part of this electric field becomes more important when the frequency increases. It then decreases again before changing its sign (between 1.9 and 2.1 eV, see Fig. 3) and reaches higher values in a short frequency range around 2.2 eV before slightly decreasing. The imaginary part of the field rapidly increases from 1.7 eV, passes through an extremum at about 2.1 eV, then decreases and changes its sign before slowly increasing again.

The results described in Fig. 3 clearly show that the metallic surface is responsible for a non-negligible surface-

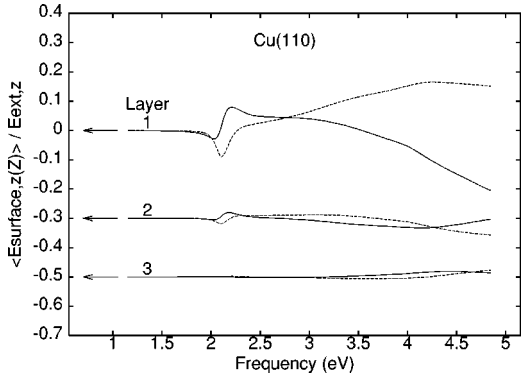

FIG. 4. Real part (solid lines) and imaginary part (dashed lines) of the averaged surface-induced electric field $\langle E_{\mathrm{surface},z}(z)\rangle$ when z is located on the atomic sites of the three top layers of the Cu(110) surface. The field, plotted as a function of frequency, is given in units of the external electric field $E_{\mathrm{ext},z}$ applied perpendicularly to the surface. The curves corresponding to different atomic layers have been translated vertically and the offsets are indicated by horizontal arrows.

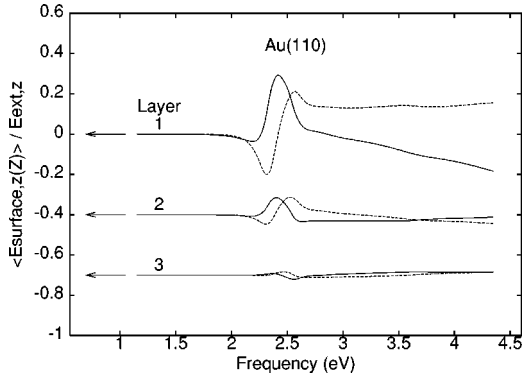

FIG. 5. As in Fig. 4 but for an Au(110) surface.

induced electric field. This field has a complex spatial variation near surface atomic sites with regions of positive and negative field. Due to the complexity of these spatial variations it is not clear how the surface-induced field will influence surface spectroscopies. We try, for this reason, to obtain a better understanding of the surface effects by investigating a spatial average of the surface-induced field. We define a locally averaged surface-induced electric field by

$$\langle \mathbf{E}_{\mathrm{surface}}(z)\rangle = (1/V)\int_{z-d/2}^{z+d/2} dz' \times \int\int_{\mathrm{unit\ cell}} dx\,dy\,\mathbf{E}_{\mathrm{surface}}(x,y,z'). \quad (13)$$

V in Eq. (13) is the volume of the parallelepiped zone where we average the surface-induced field, involving an integration in the x and y directions over the two-dimensional crystal unit cell. $\langle \mathbf{E}_{\mathrm{surface}}(z)\rangle$ directly gives the near-surface corrections to the Fresnel optics description of surface screening, and for an electric field applied perpendicularly to the surface, the locally average electric field will be given by

$$\langle E_z(z)\rangle = E_{\mathrm{ext},z} + \langle E_{\mathrm{surface},z}(z)\rangle \quad (14)$$

in the vacuum side, and by

$$\langle E_z(z)\rangle = \frac{E_{\mathrm{ext},z}}{\epsilon(\omega)} + \langle E_{\mathrm{surface},z}(z)\rangle \quad (15)$$

inside the metal. We have numerically checked that far from the surface, the bulk electric field has a spatial averaged value given by $\langle E_{\mathrm{bulk},z}(z)\rangle = E_{\mathrm{ext},z}/\epsilon(\omega)$ for any atomic site.

In Fig. 4 we present results for $\langle E_{\mathrm{surface},z}(z)\rangle$ when the point z is located at the center of an atomic site in the successive surface layers. These results show that the locally averaged surface-induced field has a significant amplitude from the interband transition threshold frequency ($\hbar\omega \approx 2.1$ eV). For $\hbar\omega < 4.5$ eV, we obtain $-0.15 < \mathrm{Re}[\langle E_{\mathrm{surface},z}(z=d/2)\rangle/E_{\mathrm{ext},z}] < 0.08$ and $-0.09 < \mathrm{Im}[\langle E_{\mathrm{surface},z}(z=d/2)\rangle/E_{\mathrm{ext},z}] < 0.16$ for an atomic site in the first layer, which clearly indicates that the surface-induced field must play an important role in the simulation of surface spectroscopy experiments. The spectral features which characterize the surface electric field are attenuated on moving towards the bulk material. For the second atomic layer and for $\hbar\omega < 4.5$ eV, we obtain an averaged surface-induced field which takes values between $-0.035E_{\mathrm{ext},z}$ and $0.021E_{\mathrm{ext},z}$ for the real part and between $-0.043E_{\mathrm{ext},z}$ and $0.014E_{\mathrm{ext},z}$ for the imaginary part. $\langle E_{\mathrm{surface},z}(z)\rangle$ is negligible by the third layer.

We have restricted our description of the near-surface electric field to the low and intermediate frequency regime, and results for higher frequencies are not shown in the present paper. Nevertheless, we mention that we observe a strong modification of the dipole moments in the top atomic layers for frequencies near $\hbar\omega = 9.26$ eV. This surface effect is due to a coupling between the *d*-electron interband transitions and the *sp*-electron bulk plasmon when the frequency approaches ω_{DP}.

B. The Au(110) surface in a perpendicular electric field

We have also investigated the surface optical properties of Au. Ignoring surface reconstruction, we find that the (110) surface presents the same kind of behavior as previously described for Cu. In particular, the spectral features observed in the near-surface field can be attributed to resonant interband transitions. The threshold for interband transitions in Au occurs at a slightly higher frequency (the bulk dipole moment shows structure at $\hbar\omega \approx 2.4$ eV). We also observe that p_{bulk} is of the same order of magnitude, but slightly more important for Au than for Cu, which should lead to more intense near-surface field effects. In Fig. 5 we present $\langle E_{\mathrm{surface},z}\rangle$ as a function of frequency, and we observe the same kind of frequency dependence as in Cu. In this case $\langle E_{\mathrm{surface},z}(z)\rangle$ can reach values as big as 30% of the external field, considerably larger than at the Cu surface.

C. The Ag(110) surface in a perpendicular electric field

We have calculated the locally averaged surface-induced electric field $\langle E_{\mathrm{surface},z}(z)\rangle$ for the Ag(110) surface. Our results, shown in Fig. 6, present a qualitatively different behav-

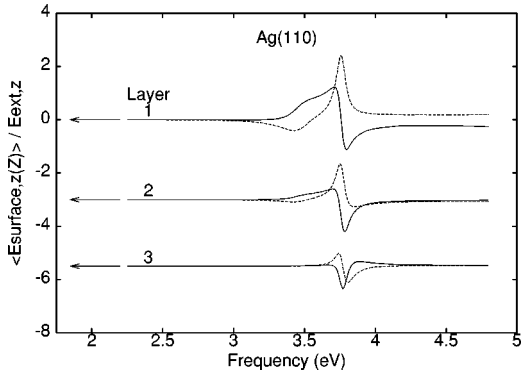

FIG. 6. As in Fig. 4 but for an Ag(110) surface.

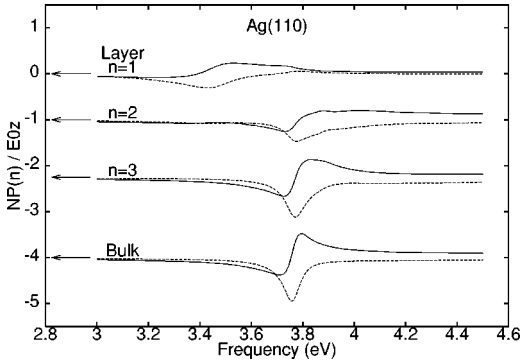

FIG. 7. Real part (solid lines) and imaginary part (dashed lines) of $Np(n)$ in units of E_{0z}, for the first ($n=1$), second ($n=2$), and third ($n=3$) atomic layers of an Ag(110) surface in a perpendicular electric field. The bulk dipole moment p_{bulk} is also shown in the figure.

ior from those of the corresponding Cu and Au surfaces. The surface induced field is much more important for Ag, for which it can reach values as large as 240, 140, and 85 % of the external field, for the top, second, and third surface layers, respectively. This surface effect also decreases more slowly than for other noble metal surfaces and it only becomes negligible from the 10th layer. The frequency dependence of $\langle E_{\mathrm{surface},z}(z)\rangle$ is characterized by two resonant features at about 3.43 and 3.76 eV, followed by a smooth tail at higher frequencies. As shown in Fig. 6, the peaked structure at 3.43 is clearly visible in the first atomic layer, considerably reduced in the second layer, and negligible from the third layer. The structure at 3.76 eV is the most important and decreases more slowly when one goes towards the bulk layers. The high frequency tail is comparable to what has been observed above the interband transition threshold for Cu and Au.

A clear physical analysis of the surface-induced electric field is more complicated for Ag than for the other noble metal surfaces. In Ag, the spectral behavior of $\langle E_{\mathrm{surface},z}(z)\rangle$ cannot be explained by the individual interband electronic excitations alone. The threshold frequency for interband transitions is estimated to occur at about 4.0 eV, and we must consider the coupling with collective excitations for a clear understanding of the peaked structures at lower frequency. The behavior of the surface-induced field may be described in terms of the dipole moments in the successive atomic layers. The strong modification of the dipole moments in the top atomic layers of an Ag surface has already been observed in Ref. 13 where the reflection amplitude has been calculated and expressed in terms of surface conductivities. These conductivities are directly related to the components of the dipole moments near the surface—-we have checked that our calculations give surface conductivities in good agreement whith those given in Ref. 13. Figure 7 shows the frequency dependence of the dipole moments in the surface, second, third, and bulk atomic layers when the external electric field is perpendicular to the Ag surface. Strong deviations from the bulk dipole moment are clearly visible at 3.43 eV in the top surface layer, and at about 3.8 eV in the second and the third layers. This suggests that the 3.43 eV peaked structure in the surface-induced electric field is due to the coupling of the applied field with surface excitations, while the structure at 3.76 eV is due to coupling with bulk excitations.

It is probably coupling to surface plasmons which is responsible for the low-frequency structure. These collective charge excitations occur at the frequency ω_{SP} for which $|\epsilon(\omega_{\mathrm{SP}})+1|\ll 1$, a condition which is satisfied at about 3.64 eV for Ag, but not for Cu or Au. This frequency is a little higher than the frequency at which we observe the surface-induced field structure, 3.43 eV, but the difference may be due to the discrete structure of the surface. In fact the coupling of the external field with surface plasmons is an artifact of the model we use—this considers the surface response to a uniform, staticlike electric field. A more elaborate model, including retardation effects and dispersion of the surface modes, would lead to the conclusion that a coupling between the optical field and the surface plasmon excitations is impossible.[26]

The resonant feature observed in Figs. 6 and 7 at 3.76 eV is due to the coupling of the external field with bulk plasmon excitations. At the bulk plasmon frequency ω_{P}, $\mathrm{Re}\{\epsilon(\omega_{\mathrm{P}})\}=0$; this condition is satisfied in all the noble metals, at $\hbar\omega_{\mathrm{P}}=3.76$, 5.76, and 8.04 eV, repectively, for Ag, Au, and Cu. The z component of the bulk dipole moment p_{bulk} is proportional to $1/\epsilon(\omega)$ [Eqs. (3) and (10)], and it will be strongly enhanced in Ag at 3.76 eV because $\mathrm{Im}(\epsilon)$ is also small at this frequency. This effect can clearly be seen in Fig. 7. A similar coupling of the external field with bulk plasmon excitations is not observed in Cu and Au because the imaginary part of the dielectric function is non-negligible at the bulk plasmon frequency for these two metals.

D. The Ag(110) surface in a parallel electric field

We now briefly describe the situation where the external electric field is applied parallel to the Ag(110) surface ($\mathbf{E}_{\mathrm{ext}}=E_{\mathrm{ext},x}\mathbf{e}_x+E_{\mathrm{ext},y}\mathbf{e}_y$). We obtain a surface-induced electric field which rapidly vanishes after a few interatomic layer distances. The results differ strongly, however, from the previous situation when we consider the spatial average of the fields: we obtain a surface-induced contribution which vanishes on average and for the electric field the numerical spatial average gives $\langle E_x(z)\rangle=E_{\mathrm{ext},x}$ and $\langle E_y(z)\rangle=E_{\mathrm{ext},y}$ for all atomic sites, including those of the first layers. We conclude

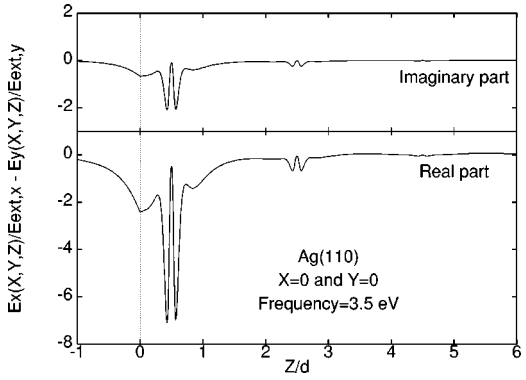

FIG. 8. Real and imaginary parts of $[E_x(x,y,z)/E_{\mathrm{ext},x} - E_y(x,y,z)/E_{\mathrm{ext},y}]$ along a [110] atomic row passing through an atom of the Ag(110) surface layer. The results are plotted versus z and for the frequency $\hbar\omega = 3.5$ eV. The jellium edge is located at $z=0$.

that when the electric field is applied parallel to the surface, the surface effects can only be observed in their local form and not on average.

As an example of these local effects of the surface response we show in Fig. 8 the difference between $E_x(x,y,z)/E_{\mathrm{ext},x}$ and $E_y(x,y,z)/E_{\mathrm{ext},y}$ along a [110] atomic row passing through an atom of the surface layer. We obtain finite values for this difference, which means that the electric field and the applied field will generally have different directions inside the metal. This is a simple consequence of the crystallographic anisotropy of Ag(110). This anisotropy persists as we go deeper inside the metal, with small amplitude oscillations for $[E_x(x,y,z)/E_{\mathrm{ext},x} - E_y(x,y,z)/E_{\mathrm{ext},y}]$. The anisotropy of the metal response is strongly enhanced in the vicinity of the metal surface and $[E_x(x,y,z)/E_{\mathrm{ext},x} - E_y(x,y,z)/E_{\mathrm{ext},y}]$ reaches its maximal values in the vicinity of the first atomic layer—see Fig. 8. Note that the anisotropy of the Ag(110) surface has been studied recently in theoretical and in experimental works, though in far-surface response.[12,13]

IV. GENERALIZATION TO METALLIC INTERFACES

The equations discussed above which describe the near-surface electric field can be generalized without any difficulty to the case of a metallic interface. For an interface between a metal 1, described by $\epsilon_{D1}(\omega)$ and $\alpha_1(\omega)$, and a metal 2, characterized by $\epsilon_{D2}(\omega)$ and $\alpha_2(\omega)$, the local electric field is given by

$$\mathbf{E}(\mathbf{r}) = \mathbf{E}_0 + \sum_{n_1} \mathsf{S}(\mathbf{r},n_1)\cdot\mathbf{p}(n_1) + \frac{\epsilon_{D1}-\epsilon_{D2}}{\epsilon_{D1}+\epsilon_{D2}} \sum_{n_1} \mathsf{S}(\mathbf{r}, -n_1)\cdot\mathbf{p}'(n_1) + \left(1+\frac{\epsilon_{D2}-\epsilon_{D1}}{\epsilon_{D2}+\epsilon_{D1}}\right)\sum_{n_2} \mathsf{S}(\mathbf{r},n_2)\cdot\mathbf{p}(n_2), \tag{16}$$

for a point $\mathbf{r}$ located in metal 1. Each term in Eq. (16) can easily be understood from the discussion in the previous sections. The field at any point on the other side of the interface is obtained from Eq. (16) by simply swapping the labels "1" and "2."

We have applied the previous equations to study an Au/Ag(111) interface. This interface has been observed in experiments and widely studied.[27] It is interesting because Ag and Au have nearly the same lattice parameters and can be grown epitaxially along the [111] axis with little change in the crystallographic characteristics of the metals. This means that the optical measurements from bulk metals can still be used to calculate the atomic site polarizability in the vicinity of this interface. We have calculated for this interface the dipole moments in successive atomic layers. Our results show a strong frequency dependence between 2.0 and 4.5 eV. The strongest deviations from the bulk dipole moments appear first at the interband transition threshold of Au (2.41 eV) and then around the Ag bulk plasmon frequency (3.76 eV). For an electric field applied perpendicular to the Au/Ag(111) interface and with the frequency $\hbar\omega = 3.76$ eV, we have obtained $|p/p_{\mathrm{bulk}}| \approx 0.88$ and $|p/p_{\mathrm{bulk}}| \approx 1.14$, respectively, for an Ag and for an Au atomic site in the interface atomic layers. This means that interface effects will be non-negligible close to the interface.

V. DISCUSSION AND CONCLUSION

The results presented in this paper have been obtained using a semiclassical model for the noble metal surface and interface. In this model, the electric charges induced in the metal are only located in a zero thickness layer at the free electron jellium edge, and inside the atomic spheres which are characterized by the position-independent polarizability $\alpha(\omega)$. More realistic results would be obtained with a much more complicated first principles calculation within the time-dependent local density approximation.[28,29] This would take into account the full atomic site response as well as the spatial extension of the induced electric charge due to the nearly free electrons. It would include the position-dependence of the atomic site polarizability, due to the modification of the electronic structure at the surface and to possible optical transitions involving localized surface states. Optical transitions between occupied and empty surface states have been observed recently in Cu(110) (Ref. 30) and Ag(110).[31,32] However, these transitions should not modify the results described in the present paper for an electric field applied perpendicular to the surface, because they correspond to electric dipoles induced in directions parallel to the surface.[33]

The semiclassical model for a noble metal surface is rather simple and does not perfectly describe the surface response. Nevertheless, we believe that it gives important indications about the near-surface field. This model is also very useful because it can be considered as complementary to the jellium model and goes beyond it. However, this simple model can be improved in several ways which are described in the following. In the semiclassical model, the dielectric response of a noble metal surface is calculated from the dielectric function of this metal and from the Drude contribution of the nearly free sp electrons. These quantities are obtained from optical measurements and for this reason the

quality of the calculated electric field directly depends on experimental data. As an example, we point out that the collision time τ characterizing the free electron gas strongly depends on the quality of the sample from which optical data are obtained. We should also mention that the dielectric function and the free electron plasmon frequency which are used in this calculation can be obtained independently of any experimental result from a first principles calculation of the bulk metal response.[34]

The induced electric charge inside each atomic site has been obtained in our model by considering a small shift of the *d*-electron charge density as described by the Roothaan-Hartree-Fock wave functions. The detailed shape of the induced local electric field depends of course on this particular choice. An alternative method would be to use wave functions calculated from a self-consistent potential of the solid. These wave functions might be more accurate if there are large environmental effects. However, we assume that the locally averaged electric field, which gives important information on surface-induced effects, does not strongly depend on this choice for the electron density.

Finally, we want to emphasize the consequences of the main results of our paper: the surface-induced electric field can be very important in some frequency range characteristic of the noble metal surface. This surface effect is confined to the top atomic layers [approximately the top three layers in the case of a Cu or Au (110) surface, the ten top layers for Ag(110)] and can be observed not only in the local electric field but also in a locally averaged field when the applied external field is perpendicular to the surface. These results show that the near-surface field should be calculated accurately when simulating surface spectroscopies. Suitable comparisons between calculated and experimental surface spectra should in this way give a measurement of near-surface local field effects. Alternatively, near-surface screening could be studied experimentally using near-field scanning optical microscopy. This method has recently been used to measure giant spatial fluctuations of the local electric field at a random metal-dielectric film.[35]

ACKNOWLEDGMENTS

This work was partially supported by the NOMOKE TMR Network, Grant No. ERBFMRXCT96-0015 and the EPSRC Grant No. GR/L33689.

*Present address: CEMES-CNRS, 29 rue Jeanne Marvig, BP 4347, 31055 Toulouse Cedex 4, France.

†Present address: Department of Physics, School of Chemistry and Physics, Keele University, Keele, Staffordshire ST5 5BG, United Kingdom.

[1] A. Liebsch, *Electronic Excitations at Metal Surfaces* (Plenum Press, New York, 1997).
[2] R. Del Sole, Phys. Status Solidi A **170**, 183 (1998).
[3] R. Del Sole, Thin Solid Films **313**, 527 (1998).
[4] P.J. Feibelman, Phys. Rev. B **14**, 762 (1976).
[5] P.J. Feibelman, Phys. Rev. B **23**, 2629 (1981).
[6] W.L. Mochán, R. Fuchs, and R.G. Barrera, Phys. Rev. B **27**, 771 (1983).
[7] W.L. Mochán and R.G. Barrera, J. Phys. (Paris) **45**, C5-207 (1984).
[8] W. Chen and W.L. Schaich, Surf. Sci. **218**, 580 (1989).
[9] A. Liebsch, J. Phys. C **19**, 5025 (1986).
[10] A. Liebsch, Phys. Rev. B **36**, 7378 (1987).
[11] K. Kempa, A. Liebsch, and W.L. Schaich, Phys. Rev. B **38**, 12 645 (1988).
[12] J. Tarriba and W.L. Mochán, Phys. Rev. B **46**, 12 902 (1992).
[13] Y. Borensztein, W.L. Mochán, J. Tarriba, R.G. Barrera, and A. Tadjeddine, Phys. Rev. Lett. **71**, 2334 (1993).
[14] A. Liebsch and W.L. Schaich, Phys. Rev. B **52**, 14 219 (1995).
[15] W.L. Schaich and W. Chen, Phys. Rev. B **89**, 10 714 (1989).
[16] M. Fluchtmann, S.B.D. Kellen, J. Braun, and G. Borstel, Surf. Sci. **404**, 663 (1998).
[17] D. Samuelsen and W. Schattke, Phys. Rev. B **51**, 2537 (1995).
[18] P.B. Johnson and R.W. Christy, Phys. Rev. B **6**, 4370 (1972).
[19] J. H. Weaver, C. Krafka, D. W. Lynch, and E. E. Koch, *Physics Data Series* (Fachsinformationszentrum-Energie, Physik, Mathematik, Karlsruhe, 1981).
[20] D.E. Aspnes, Am. J. Phys. **50**, 704 (1982).
[21] B.M.E. Van Der Hoff and G.C. Benson, Can. J. Phys. **31**, 1087 (1953).
[22] F.W. De Wette and G.E. Schacher, Phys. Rev. **137**, A78 (1965).
[23] N. Kar and A. Bagchi, Solid State Commun. **33**, 645 (1980).
[24] E. Clementi and C. Roetti, At. Data Nucl. Data Tables **14**, 177 (1974).
[25] N. W. Ashcroft and N. D. Mermin, *Solid State Physics* (Saunders College Publishing, Philadelphia, 1976).
[26] F. García-Moliner and F. Flores, *Introduction to the Theory of Solid Surfaces* (Cambridge University Press, Cambridge, 1979).
[27] R.J. Culbertson, L.C. Feldman, P.J. Silverman, and H. Boehm, Phys. Rev. Lett. **47**, 657 (1981).
[28] H. Ishida and A. Liebsch, Phys. Rev. B **45**, 6171 (1992).
[29] G. Onida, R. Del Sole, M. Palummo, O. Pulci, and L. Reining, Phys. Status Solidi A **170**, 365 (1998).
[30] Ph. Hofmann, K.C. Rose, V. Fernandez, A.M. Bradshaw, and W. Richter, Phys. Rev. Lett. **75**, 2039 (1995).
[31] J.K. Hansen, J. Bremer, and O. Hunderi, Surf. Sci. **418**, L58 (1998).
[32] K. Stahrenberg, T. Herrmann, N. Esser, J. Sahm, W. Richter, S.V. Hoffmann, and Ph. Hofmann, Phys. Rev. B **58**, R10 207 (1998).
[33] M.J. Yiang, G. Pajer, and E. Burstein, Surf. Sci. **242**, 306 (1991).
[34] N.E. Christensen and B.O. Seraphin, Phys. Rev. B **4**, 3321 (1971).
[35] S. Gresillon, L. Aigouy, A.C. Boccara, J.C. Rivoal, X. Quelin, C. Desmarest, P. Gadenne, V.A. Shubin, A.K. Sarychev, and V.M. Shalaev, Phys. Rev. Lett. **82**, 4520 (1999).